

# The anomalous behavior of coefficient of normal restitution in the oblique impact

Hiroto Kuninaka<sup>1,\*</sup> and Hisao Hayakawa<sup>2</sup>

<sup>1</sup>*Graduate School of Human and Environmental Studies,  
Kyoto University, Sakyo-ku, Kyoto, Japan, 606-8501*

<sup>2</sup>*Department of Physics, Yoshida-south campus, Kyoto University, Sakyo-ku, Kyoto, Japan, 606-8501*  
(Dated: February 14, 2019)

The coefficient of normal restitution in an oblique impact is theoretically studied. Using a two-dimensional lattice models for an elastic disk and an elastic wall, we demonstrate that the coefficient of normal restitution can exceed one and have a peak against the incident angle in our simulation. Finally, we explain these phenomena based upon the phenomenological theory of elasticity.

The coefficient of restitution (COR)  $e$  is introduced to determine the post-collisional velocity in the normal collision of two materials in elementary physics. COR is defined by

$$\mathbf{u}' \cdot \mathbf{n} = -e \mathbf{u} \cdot \mathbf{n}, \quad (1)$$

where  $\mathbf{u}$  and  $\mathbf{u}'$  are respectively the relative velocity of the contact point of two colliding materials before and after collision, and  $\mathbf{n}$  is the normal unit vector of the tangential plane of them. Though many text books of elementary physics state that  $e$  is a material constant, many experiments and simulations show that  $e$  decreases as the impact velocity increases[1]. The dependence of  $e$  on the low impact velocity are theoretically treated by the quasi-static theory [2, 3, 4].

While COR has been believed to be less than 1 in most situations, it is recently reported that COR can exceed 1 in oblique impacts[5, 6, 7]. In particular, Louge and Adams[7] reported that COR increases as a linear function of the magnitude of  $\tan \gamma$  in the oblique impact of a hard aluminum oxide sphere on a thick elastoplastic plate with the incident angle  $\gamma$ . Young's modulus of the wall is 100 times softer than that of the sphere in the experiment. They also suggested COR can exceed 1 in most grazing impacts. This anomalous behavior is novel and interesting.

In this letter, we demonstrate that COR increases with  $\tan \gamma$  to exceed 1 at the critical incident angle through in our two-dimensional simulation of the oblique impact between an elastic disk and an elastic wall. Finally, we explain our results with the aid of the theory of elasticity[8].

Let us introduce our numerical model[9]. Our numerical model consists of an elastic disk and an elastic wall (Fig. 1). The width and the height of the wall are  $8R$  and  $2R$ , respectively, where  $R$  is the radius of the disk. We adopt the fixed boundary condition for the both side ends and the bottom of the wall. To make each of them, at first, we place mass points at random in a circle and a rectangle with the same density, respectively. For the disk, we place 800 particles at random in a circle with the radius  $R$  while for the wall, similarly, we place 4000 particles at random in a rectangle.

After that, we connect all mass points with nonlinear

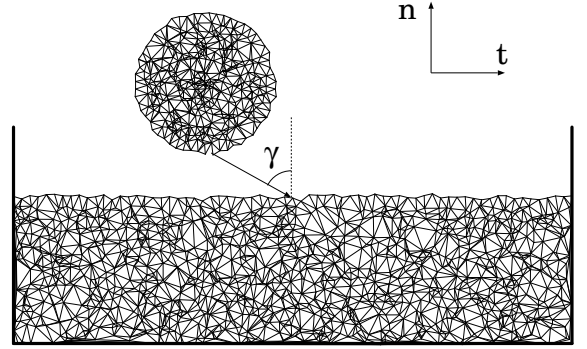


FIG. 1: The elastic disk and wall consisted of random lattice.

springs for each of them using the Delaunay triangulation algorithm[10]. The spring interaction between connected mass points is given by

$$V^{(i)}(x) = \frac{1}{2}k_a^{(i)}x^2 + \frac{1}{4}k_b^{(i)}x^4, \quad i = d(\text{disk}), w(\text{wall}), \quad (2)$$

where  $x$  is a stretch from the natural length of spring, and  $k_a^{(i)}$  and  $k_b^{(i)}$  are the spring constants for the disk( $i=d$ ) and the wall( $i=w$ ). In most of our simulations, we adopt  $k_a^{(d)} = 1.0 \times mc^2/R^2$  for the disk while  $k_a^{(w)} = k_a^{(d)}/100$  for the wall, where  $m$  and  $c$  are the mass of each mass point and the one-dimensional velocity of sound, respectively. In this model, the wall is much softer than the disk as in Ref.[7]. We adopt  $k_b^{(i)} = k_a^{(i)} \times 10^{-3}/R^2$  for each of them. We do not introduce any dissipation mechanism in this model. The interaction between the disk and the wall during a collision is given by  $\mathbf{F}(l) = aV_0 \exp(-al)\mathbf{n}^s$ , where  $a$  is  $300/R$ ,  $V_0$  is  $amc^2R/2$ ,  $l$  is the distance between each surface particle of the disk and the surface spring of the wall, and  $\mathbf{n}^s$  is the normal unit vector to the spring.

In this model, roughness of the surfaces is important to make the disk rotate after collisions[9]. To make rough-

ness, we displace the surface particles of the disk and the wall by generating normal random numbers with its average is 0 and its standard deviation is  $\delta = 3 \times 10^{-2}R$ . All the data in this paper are obtained from the average of 100 samples in random numbers.

Poisson's ratio  $\nu$  and Young's modulus  $E$  of this model can be evaluated from the strains of the band of random lattice in vertical and horizontal directions to the applied force. We obtain Poisson's ratio  $\nu$  and Young's modulus  $E$  as  $\nu = (7.50 \pm 0.11) \times 10^{-2}$  and  $E = (9.54 \pm 0.231) \times 10^3 mc^2/R^2$ , respectively.

In our simulation, we define the incident angle  $\gamma$  by the angle between the normal vector of the wall and the initial velocity vector of the disk (see Fig. 1). We fix the initial colliding speed of the disk as  $|\mathbf{v}(0)| = 0.1c$  to control the normal and tangential components of the initial colliding velocity as  $v_t(0) = |\mathbf{v}(0)| \sin \gamma$  and  $v_n(0) = |\mathbf{v}(0)| \cos \gamma$ , respectively. From the normal components of the contact point velocities before and after a collision, we calculate COR for each  $\gamma$ . We use the fourth order symplectic numerical method for the numerical scheme of integration with the time step  $\Delta t = 10^{-3}R/c$ .

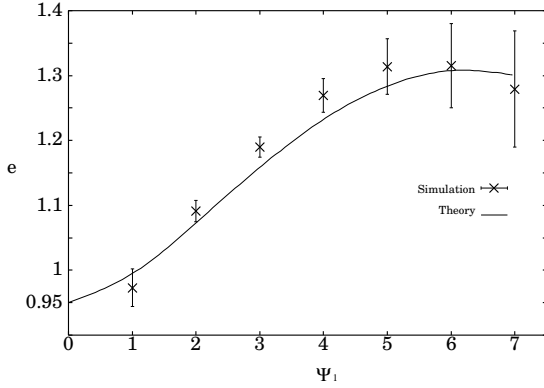


FIG. 2: Numerical and theoretical results of the relation between  $\Psi_1$  and COR.

Figure 2 is COR against the tangent of the incident angle  $\Psi_1 = \tan \gamma$  by our model. The cross points are the average and the error bars are the standard deviation of 100 samples for each incident angle. This result shows that COR increases as  $\Psi_1$  increases to exceed 1, and has a peak around  $\Psi_1 = 6.0$ . This behavior is contrast to that in the experiment by Louge and Adams[7].

Here, let us clarify the mechanism of our results. Louge and Adams[7] interpreted that  $e$  exceeds 1 in association with the local deformation on the surface of the thick wall during an impact. They attribute their results to the rotation of normal unit vector of the wall surface by an angle  $\alpha$  and derive the corrected expression for COR. Thus, we determine the quantity of  $\alpha$  at each incident angle from the theory of elasticity and calculate corrected COR.

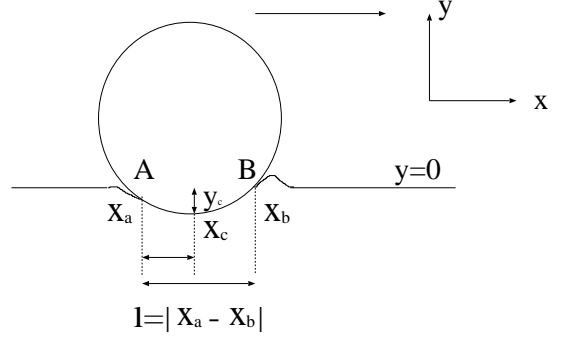


FIG. 3: The schematic figure of a hard disk sliding on a soft wall.  $x$  coordinates of both ends of the contact area AB are  $x = x_a$  and  $x = x_b$ .

Figure 3 is the schematic figure of a hard disk moving from left to right on a wall, where the length of the contact area is  $l = |x_b - x_a|$ . We assume that the contact area is small in comparison with the radius of the disk  $R$ , and the contact area can be approximated by the parabola

$$f(x) = (x - x_c)^2/2R + y_c, \quad (3)$$

where  $(x_c, y_c)$  corresponds to the contact point of the disk. We define the corrected angle  $\alpha$  as the angle between the line segment AB and the tangential unit vector  $\mathbf{t}$  which is horizontal to the wall surface. Thus,  $\tan \alpha$  is given by

$$\tan \alpha \equiv \frac{f(x_b) - f(x_a)}{l}. \quad (4)$$

To calculate Eq.(4), we need the ratio of  $|x_c - x_a|$  to  $l$  because the left and the right sides of the contact area are not equal due to the frictional force. From the theory of elasticity[8, 11], this ratio can be estimated as

$$\frac{x_c - x_a}{l} = 1 - \theta \quad \text{with} \quad \theta = \frac{1}{\pi} \arctan \frac{1 - 2\nu}{\mu(2 - 2\nu)}, \quad (5)$$

where  $\nu$  is Poisson's ratio of the wall and  $\mu$  is the coefficient of friction. Note that Eq.(5) equals to 1/2 when  $\mu = 0$ . From Eqs.(4) and (5),  $\tan \alpha$  is reduced to

$$\tan \alpha = \frac{1 - 2\theta}{2 - 2\theta} \frac{|x_c - x_a|}{R}. \quad (6)$$

In Eq.(6),  $|x_c - x_a|$  can be evaluated by the simulation data. From our simulation, the maximum value of  $y_c$  is about  $0.17R$  at  $\Psi_1 = 1.0$ . Assuming the disk is pressed in the normal direction, we can estimate the contact area as about  $1.1R$  which is the maximum value. Thus, we adopt its half value,  $0.55R$ , as  $|x_c - x_a|$ .

The coefficient of friction  $\mu$  in  $\theta$  is defined through

$$\mu = |\mathbf{n} \times \mathbf{J}|/(\mathbf{n} \cdot \mathbf{J}) = |J_t|/|J_n| \quad (7)$$

with the impulse imparted by the disk  $\mathbf{J} = m(\mathbf{v}' - \mathbf{v})$ , where  $\mathbf{v}$  and  $\mathbf{v}'$  are the velocities of center of mass before and after collision, respectively. Cross points in Fig.4 is  $\mu$  calculated from our simulation data against each  $\Psi_1$ . Figure 4 shows  $\mu$  has a peak at  $\Psi_1 = 3.0$ . Substituting this result to Eqs.(5) and (6), we obtain the relation between  $\Psi_1$  and  $\tan \alpha$ .

Next, we calculate the corrected COR by  $\tan \alpha$ . We define  $\mathbf{n}^\alpha$  and  $\mathbf{t}^\alpha$  which are rotated toward the incoming disk by  $\alpha$  from  $\mathbf{n}$  and  $\mathbf{t}$ , respectively. The impulse  $\mathbf{J}$  is represented as

$$\mathbf{J} = J_n \mathbf{n} + J_t \mathbf{t} = J_n^\alpha \mathbf{n}^\alpha + J_t^\alpha \mathbf{t}^\alpha. \quad (8)$$

Thus,  $J_n$  and  $J_t$  are expressed as  $J_n = J_n^\alpha \cos \alpha + J_t^\alpha \sin \alpha$  and  $J_t = -J_n^\alpha \sin \alpha + J_t^\alpha \cos \alpha$ . From Eq.(7),  $\mu$  is calculated as

$$\mu = \frac{\mu^\alpha - \tan \alpha}{1 + \mu^\alpha \tan \alpha}, \quad (9)$$

where  $\mu^\alpha = |J_t^\alpha|/|J_n^\alpha|$  which is the coefficient of sliding friction without deformation of the wall (Note that  $\mu = \mu^\alpha$  when  $\alpha = 0$ ). A similar expression is derived by Louge and Adams[7].

Similarly, we express  $\mathbf{u}$  and  $\mathbf{u}'$  which are the velocities of the contact point of the disk before and after collision as  $\mathbf{u} = u_n \mathbf{n} + u_t \mathbf{t} = u_n^\alpha \mathbf{n}^\alpha + u_t^\alpha \mathbf{t}^\alpha$  and  $\mathbf{u}' = u_n' \mathbf{n} + u_t' \mathbf{t} = u_n'^\alpha \mathbf{n}^\alpha + u_t'^\alpha \mathbf{t}^\alpha$ . From these expressions, we can calculate the observed COR  $e = -u_n'/u_n$  and COR without deformation of the wall  $e^\alpha = -u_n'^\alpha/u_n^\alpha$ . From these definitions, we obtain

$$e = \frac{e^\alpha + \Psi_2^\alpha \tan \alpha}{1 - \Psi_1^\alpha \tan \alpha}, \quad (10)$$

where  $\Psi_1^\alpha = -u_t^\alpha/u_n^\alpha$  and  $\Psi_2^\alpha = -u_t'^\alpha/u_n^\alpha$ . By noting that  $u_t^\alpha = u_n \sin \alpha + u_t \cos \alpha$  and  $u_n^\alpha = u_n \cos \alpha - u_t \sin \alpha$ , we can express  $\Psi_1^\alpha$  as

$$\Psi_1^\alpha = (\Psi_1 - \tan \alpha)/(1 + \Psi_1 \tan \alpha). \quad (11)$$

On the other hand, in the oblique impact of hard disks accompanied by gross slip on the surface,  $\Psi_2^\alpha$  is represented by

$$\Psi_2^\alpha = \Psi_1^\alpha - 3(1 + e^\alpha)\mu^\alpha \quad (12)$$

in the two-dimensional situation[12].  $\mu^\alpha$  in Eq.(12) is a function of  $\mu$  and  $\tan \alpha$ . To draw the solid line in Fig.2, at first, we calculate  $\tan \alpha$  and  $\mu$  by Eqs.(6) and (7) respectively for each  $\Psi_1$ . After that, we calculate  $\Psi_1^\alpha$  and  $\Psi_2^\alpha$  by Eqs.(11) and (12), and obtain  $e$  by substituting them into Eq.(10) for each  $\Psi_1$ . We assume  $e^\alpha$  is a constant less than 1. The solid line of Fig.2 is Eq.(10) with  $e^\alpha = 0.95$  which is the value in the normal impact. All points are interpolated with cubic spline interpolation method to draw the theoretical curve. Such a theoretical description of  $e$  is qualitatively consistent with our numerical

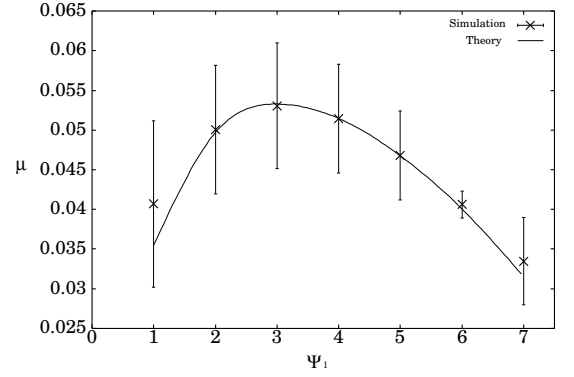


FIG. 4: Numerical and theoretical results of the relation between  $\Psi_1$  and  $\mu$ .

result, though the theoretical value is smaller than the observed value. As can be seen, COR  $e$  depends on the relation between  $\mu$  and  $\Psi_1$ .

Finally, we explain the dependence of  $\mu$  upon  $\Psi_1$ . In our model, the roughness on the surfaces of the wall and the disk are important to generate rotational motion of the disk after collision[9]. We assume that the tangential velocity of the disk is decreased by  $\eta$  when the disk interacts with one jag on the surface of the wall. The length  $l$  that the disk slides within the duration  $\tau$  is expressed as  $l \simeq v_t(0)\tau \simeq v_t(0)\pi(R/c)\sqrt{\ln(4c/v_n(0))}$ , where we use the expression of  $\tau$  based on the theory of elasticity[13]. Assuming that jag are placed on the surface of the wall uniformly and have same size, the tangential velocity after collision is calculated as  $v_t(\tau) = v_t(0) - \eta\rho v_t(0)\pi(R/c)\sqrt{\ln(4c/v_n(0))}$ , where  $\rho$  is the number of jags on the unit length. Noting that  $v_t(0) = |\mathbf{v}(0)| \sin \gamma$  and  $v_n(0) = |\mathbf{v}(0)| \cos \gamma$ , the tangential impulse  $J_t$  is

$$J_t = -m\eta\rho|\mathbf{v}(0)| \sin \gamma \pi \frac{R}{c} \sqrt{\ln \left( \frac{4c}{|\mathbf{v}(0)| \cos \gamma} \right)}. \quad (13)$$

On the other hand, the normal impulse is given by  $J_n = -m(e+1)|\mathbf{v}(0)| \cos \gamma$ , where we use  $v_n(\tau) = -ev_n(0)$ . We assume that the tangential impulse decreases by  $J_t'$  which is proportional to the tangential velocity resulting from the effect of the local deformation of the wall.  $J_t'$  is expressed as  $J_t' = -m\zeta|\mathbf{v}(0)| \sin \gamma$ , where  $\zeta$  is a proportionality constant. Thus,  $\mu$  can be represented by the ratio of  $|J_t - J_t'|$  to  $|J_n|$  as

$$\mu = \left| \zeta \tan \gamma - \eta\rho \tan \gamma \pi \frac{R}{c} \sqrt{\ln \left( \frac{4c}{|\mathbf{v}(0)| \cos \gamma} \right)} \right| / (e+1). \quad (14)$$

In this expression,  $e$  is the cross point in Fig.(2) for each  $\Psi_1 = \tan \gamma$ .  $\zeta$  and  $\eta$  are fitting parameters. Assuming that the disk rotates scarcely after collision, we calculate Eq.(14) by the contact point velocity  $\mathbf{u}$  instead of  $\mathbf{v}$ .

The solid curve in Fig.(4) is Eq.(14) with fitting parameters,  $\zeta = 0.397$  and  $\eta\rho = 0.163c/R$ . Eq.(14) shows good agreement with our numerical result. We do not claim that our simple theory reproduces the experimental result because of a lot of fitting parameters. However, we would like to emphasize that our picture for the relation between  $\mu$  and  $\Psi_1$  captures the essence of the physics of impact.

For discussion, firstly, we refer to the origin of the relation between  $e$  and  $\Psi_1$ . As described previously, for  $e$  to exceed 1, it is essential for the wall surface to deform locally, which produces the rotation of the normal unit vector to the wall surface. If  $\alpha = 0$  in Eq.(10),  $e$  is equal to  $e^\alpha$  which is a constant less than 1. We have also carried out the simulation when  $k_a^{(w)} = 10 \times k_a^{(d)}$ , which means the wall is harder than the disk. In this case,  $e$  takes almost constant value to exceed 1 abruptly at  $\Psi_1 = 4.5$ . This tendency resembles the experiment by Calsamiglia *et al.*[6]. This result can be attributed to the insufficient local deformation originated in the hardness of the wall. Thus, for  $e$  to increase smoothly to exceed 1, the wall should be smaller than the disk to generate enough deformation. In addition, it is important to fix the initial kinetic energy of the disk. we have confirmed so far that  $e$  does not exceed 1 when  $\Psi_1$  is controlled by the change of  $v_t$  with fixed  $v_n$ [9]. In that case, the initial kinetic energy of the disk becomes large in the large  $\Psi_1$  so that the local deformation of the wall is easy to collapse in the grazing collision.

Secondly, the initial velocity of the disk and the local deformation of the wall are so large that the local dissipation in springs and gravity have not affected our numerical results. In addition, we have carried out other simulation with a disk of 400 particles and a wall of 2000 particles to investigate the effect of the model size. Although there is a slight difference between the results, the data can be also reproduced quite well by our phenomenological theory.

Thirdly, the local deformation of the wall also affects the relation between  $\mu$  and  $\Psi_1$ . In early studies, it has been shown that  $\mu$  depends on the impact velocity [7, 14]. In our simulation, the magnitude of  $\alpha$  has a peak around  $\Psi_1 = 3.0$ . This behavior is interpreted as that the local deformation collapses with large  $v_t$ . We derived in this letter the relation between  $\mu$  and  $\Psi_1$  by Eq.(14). By controlling  $\zeta$  and  $\eta$ , Eq.(14) shows monotonous increase like the result of Louge and Adams[7]. The difference between the results of their experiment and our simulation may be explained by the choice of these parameters.

Finally, we adopt the static theory of elasticity to explain our numerical results in this letter. However, it is important to solve the time-dependent equation of the deformation of the wall surface to analyze the dynamics of impact phenomena. The dynamical analysis is our

future task.

In summary, we have carried out the two-dimensional simulation of the oblique impact of an elastic disk on an elastic wall. We have found that COR can exceed 1 in the oblique impact, which is attributed to the local deformation of the wall. We have estimated the magnitude of the local deformation  $\alpha$  based upon the static theory of elasticity and derived the relation between  $e$  and  $\Psi_1$  by taking into account the rotation of the normal unit vector of the wall surface. The relation between  $\mu$  and  $\Psi_1$  is also related to the local deformation and explained by the simple analysis assuming the decrease of the tangential impulse proportional to the initial tangential velocity of the disk.

We would like to thank Y. Tanaka and S. Nagahiro for their valuable comments. We would also like to thank Prof. M. Y. Louge for his detailed introduction of their experiment to us and some valuable comments. Parts of numerical computation in this work were carried out at Yukawa Institute Computer Facility. This study is partially supported by the Grant-in-Aid of Ministry of Education, Science and Culture, Japan (Grant No. 15540393).

---

\* E-mail: kuninaka@yuragi.jinkan.kyoto-u.ac.jp

- [1] W. J. Stronge, *Impact Mechanics* (Cambridge University Press, Cambridge, 2000).
- [2] G. Kuwabara and K. Kono, Jpn. J. Appl. Phys. **26**, 1230 (1987).
- [3] W. A. Morgado and I. Oppenheim, Phys. Rev. E **55**, 1940 (1997).
- [4] J.-M. H. N. Brilliantov, F. Spahn and T. Pöschel, Phys. Rev. E **53**, 5382 (1996).
- [5] C. E. Smith and P.-P. Liu, J. of Appl. Mech. **59**, 963 (1992).
- [6] J. Calsamiglia, S. W. Kennedy, A. Chatterjee, A. Ruina, and J. T. Jenkins, J. of Appl. Mech. **66**, 146 (1997).
- [7] M. Y. Louge and M. E. Adams, Phys. Rev. E **65**, 021303 (2002).
- [8] L. A. Galin, *Contact problems in the theory of elasticity* (Gostekhizdat, Moscow, 1953).
- [9] H. Kuninaka and H. Hayakawa, J. Phys. Soc. Jpn. **72**, 1655 (2003).
- [10] K. Sugihara, *Data Structure and Algorithms(in Japanese)* (Kyoritsu, Japan, 2001).
- [11] D. A. Hills, D. Nowell, and A. Sackfield, *Mechanics of Elastic Contacts* (Butterworth-Heinemann, Oxford, 1993).
- [12] O. R. Walton and R. L. Braun, J. Rheol. **30**, 949 (1986).
- [13] H. Hayakawa and H. Kuninaka, Chem. Eng. Sci. **57**, 239 (2002).
- [14] D. A. Gorham and A. H. Kharaz, Powder Technology **112**, 193 (2000).